

Window-Region Longwave Fluxes: Accounting for Cloud Scattering

*E.E. Takara and R.G. Ellingson
Department of Meteorology
University of Maryland
College Park, Maryland*

Introduction

The longwave radiative transfer models used in many general circulation models (GCMs) assume that broken cloud fields consist of flat black plates. This neglects individual cloud geometry and cloud optical properties (i.e., single scattering albedo). The error due to neglecting cloud geometry has been well documented (Ellingson 1982; Harshvardhan and Weinman 1982; Killen and Ellingson 1994). Recently, Takara and Ellingson (1996) showed that cloud longwave scattering effects could have the same magnitude as geometric effects if gaseous absorption is neglected. We extend the investigation of cloud longwave scattering effects by allowing gaseous absorption.

Flux Computation

There is significant variation in gaseous absorptivity across the 8-12 μm window. As a result, the upward flux above the cloud field and the downward flux below the cloud field were computed by adding the fluxes computed over six spectral intervals:

$$F^{\uparrow} = \int_{8 \mu\text{m}}^{12 \mu\text{m}} F_{\lambda}^{\uparrow} d\lambda = \sum_{i=1}^6 F_i^{\uparrow} \delta\lambda \quad (1)$$

The intervals were chosen to emphasize the spectral features of the lowest kilometer of the atmosphere. The intervals are

$$\begin{aligned} 8.00 \mu\text{m} < \lambda_1 < 8.25 \mu\text{m}; & 8.25 \mu\text{m} < \lambda_2 < 8.75 \mu\text{m}; \\ 8.75 \mu\text{m} < \lambda_3 < 9.25 \mu\text{m}; & 9.25 \mu\text{m} < \lambda_4 < 10.0 \mu\text{m}; \\ 10.0 \mu\text{m} < \lambda_5 < 11.0 \mu\text{m}; & 11.0 \mu\text{m} < \lambda_6 < 12.0 \mu\text{m} \end{aligned}$$

The fluxes in the spectral intervals were computed using the Monte Carlo method. Photon bundles were emitted from planar surfaces above and below the cloud fields and tracked until absorption. The probabilities of gaseous absorption and cloud intersection were calculated using the line-by-line

radiative transfer model (LBLRTM) code and the probability of clear line of sight (PCLoS) used in Ellingson.

The LBLRTM code was used to calculate $T(Z_i, Z_j, \theta)$ the transmissivity between altitude Z_i and Z_j at zenith angle θ . Since transmissivities range between zero and one they can be directly used to model transmission/absorption. If ζ is a random number between zero and one, then

$$\zeta \leq T(Z_i, Z_j, \theta) \text{ bundle transmitted} \quad (2a)$$

$$\zeta > T(Z_i, Z_j, \theta) \text{ bundle absorbed} \quad (2b)$$

Assume that after N different bundles are tested for absorption, M are absorbed. As N increases, M/N will approach $1 - T(Z_i, Z_j, \theta)$. Having pre-calculated values for transmissivity makes modeling gaseous absorption quite simple in the Monte Carlo method.

In Ellingson, the PCLoS for a broken cloud field composed of a single layer of randomly overlapping, identical, cylinders for a specified zenith angle (θ) was given as

$$\begin{aligned} \text{PCLoS}(\theta) &= (1 - N) \exp(-b \tan \theta); \\ b &= -\frac{2\beta \ln(1 - N)}{\pi} \end{aligned} \quad (3)$$

where β is the ratio of cylinder height to radius (H/R). The PCLoS was used to determine if the bundle intersects the clouds. If χ is a random number between zero and one then

$$\chi \leq \text{PCLoS} \text{ bundle does not intersect the clouds} \quad (4a)$$

$$\chi > \text{PCLoS} \text{ bundle intersects the clouds} \quad (4b)$$

To compute the flux at some altitude, the photon bundles are emitted at a randomly determined zenith angle (θ) with a random absorption probability (ζ) and intersection probability

(χ). Given θ , χ and ζ Equations 4a,b and 2a,b are used to determine if the bundle intersects a cloud or is absorbed. If the bundle intersects a cloud, it is tracked within the cloud until it is absorbed or escapes the cloud. If the bundle escapes the cloud tracking resumes with Equation 4a,b and 2a,b.

Assumptions and Parameters

Four assumptions were made in the Monte Carlo computations. First, the cloud field was a single layer of identical, randomly overlapping, cylinders with a constant cloud base altitude. Second and third, the clouds were homogenous with the same temperature profile as the surrounding air. Lastly, because the cloud/droplet optical thickness was several orders of magnitude larger than that of the gases, gaseous absorption within the cloud was ignored.

The fluxes were computed for various cloud aspect ratio-cloud (α = cloud height/cloud diameter) diameter pairs, base cloud fraction (N), and cloud base altitude (Z_b). To model small flat clouds, $\alpha = 0.5$ with a diameter of 0.25 km was chosen. To model larger tall clouds, $\alpha = 1.0$ with a diameter of 1.0 km was used. The values of N were 0.1, 0.3, 0.5, 0.7, 0.9, and 1.0. Values of Z_b were 0.5, 2.0, 4.0, and 10 km.

The cloud extinction coefficient (K_t), single scattering albedo (ω_0), and asymmetry factor (g) within each wavelength interval were calculated from the parameterizations of Hu and Stamnes (1993).

$$\frac{K_t}{LWC} = a_1 (R_{eq})^{b_1} + c_1 \quad (5a)$$

LWC is the cloud liquid water content in (g m^{-3}); K_t has the units m^{-1} .

$$\omega_0 = a_2 (R_{eq})^{b_2} + C_2 \quad (5b)$$

$$g = a_3 (R_{eq})^{b_3} + C_3 \quad (5c)$$

Values for R_{eq} were 5 and 10 μm ; $LWC = 0.1, 1 \text{ g m}^{-3}$. Values for K_t , ω_0 , and g for $LWC = 0.1 \text{ g m}^{-3}$ are shown in Figure 1. This increase in forward scattering will tend to reduce scattering effects, making the cloud act more like a blackbody.

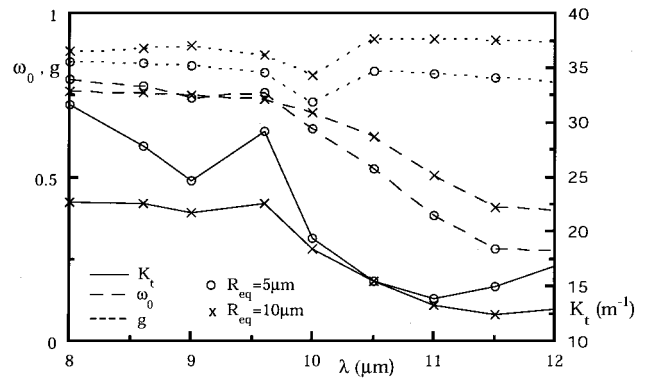


Figure 1. Cloud optical properties.

Results

The fluxes at the surface and at 15 km for $R_{eq} = 5, 10 \mu\text{m}$; $LWC = 1 \text{ g m}^{-3}$ are shown in Figure 2. The fluxes for $LWC = 0.1 \text{ g m}^{-3}$ are not shown because there is little difference from $LWC = 1.0 \text{ g m}^{-3}$. Note that the fluxes decrease with cloud base altitude and that the fluxes for clouds with the same base altitude converge to the same completely overcast ($N = 1$) flux, except for $F^{\uparrow}_{Z_b} = 0.5 \text{ km}$. This is the result of the vertical resolution of the model. The 750 m difference in height between the top of the 0.25-km cloud and the top of the

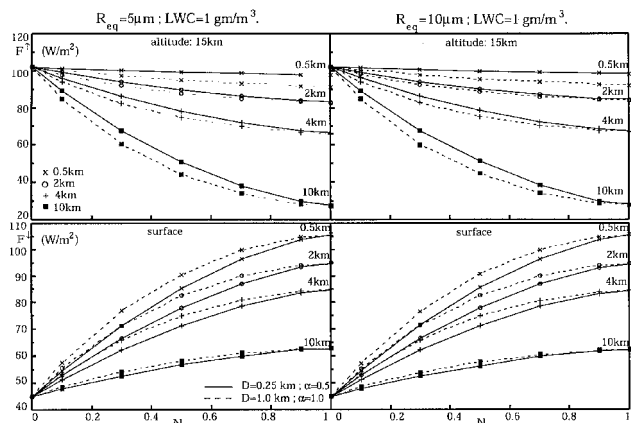


Figure 2. Upward flux at 15 km and downward flux at surface.

1-km cloud was within the model gridding except for the case of $Z_0 = 0.5$ km. The vertical resolution can be increased for future studies.

The absolute and percentage error from the flat plate approximation when $R_{eq} = 10 \mu\text{m}$ is shown in Figure 3. As shown in Takara and Ellingson, the flat plate errors are quite large and are largest for values of N around 0.5. This indicates the error due to neglecting geometry is larger than the error due to neglecting optical properties.

The surface flux error in assuming clouds are black (the geometric black cloud approximation) is shown in Figure 4. The error in the flux at the surface is less than 2 W m^{-2} and 3%; as noted previously, the cloud becomes “blacker” as R_{eq} increases. The errors are significantly smaller than the 16 W m^{-2} and 45% errors shown in Takara and Ellingson. This difference can be attributed to gaseous absorption/emission, especially from the lowest kilometer of the atmosphere. Since the atmosphere in Takara and Ellingson was nonparticipating, the clear sky downward flux was zero; the downward flux reflected from 10 km clouds was 25 W m^{-2} . Here, the clear sky downward flux is 45 W m^{-2} and the 10 km cloud flux is 62 W m^{-2} . While the absolute difference between the clear and cloudy fluxes is comparable, the relative difference is much smaller. The participating atmosphere also reduces the flux reflected downward in two ways. First, the energy that reaches the clouds is reduced. Second, it absorbs the energy reflected from the clouds before it reaches the surface.

The geometric black cloud error for upward flux error at 15 km is shown in Figure 5. The errors are less than 4 W m^{-2} and 6%; the black cloud approximation improves

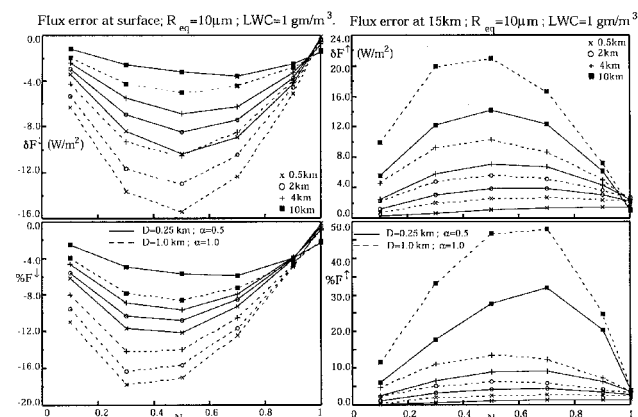


Figure 3. Error for flat black plate approximation.

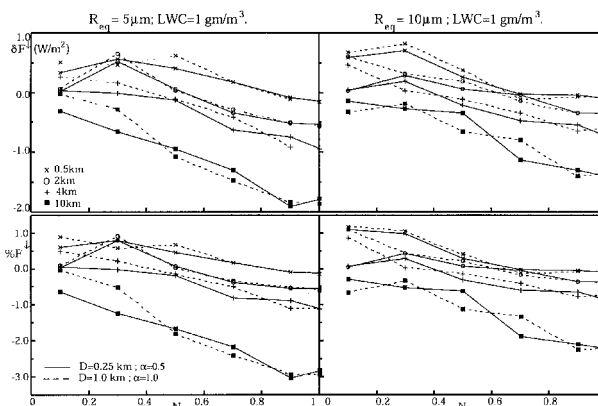


Figure 4. Error in geometric black cloud approximation for surface flux.

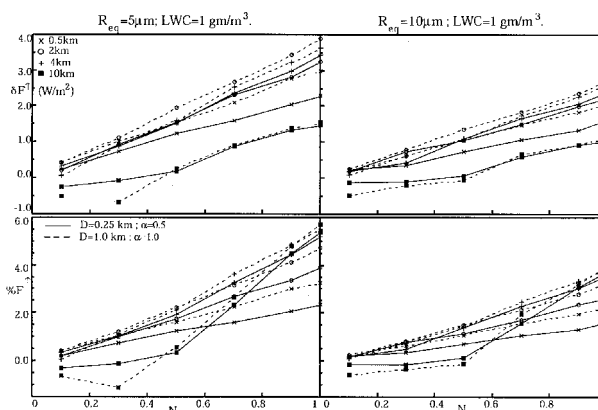


Figure 5. Error in geometric black cloud approximation for upward flux at 15 km.

as R_{eq} increases. Again, the errors are lower than those predicted by Takara and Ellingson; the error for reflecting low cloud fields was 1.5 W m^{-2} and 1.8%. Once more, the difference is primarily due to the participation of the lowest kilometer of the atmosphere.

The emission of the first kilometer negates the reduction in emission from a scattering cloud.

Summary and Conclusions

For the cases considered, geometric effects are more important than scattering effects. The geometric black cloud approximation was accurate. The relatively small error can be

attributed to the masking effect of gaseous absorption/emission, especially the lowest kilometer of the atmosphere. Cloud scattering effects are most apparent for fluxes at higher altitudes. As the cloud droplet size increased, cloud scattering effects decreased because the asymmetry factor increased with droplet size. The flat black plate approximation is inadequate for the cases considered. While scattering effects are not significant for the fluxes presented, additional cases should be considered.

In particular, clouds with smaller droplets and lower water contents should be examined. In future work, additional cloud optical parameterizations will be examined as well as other cloud field PCLoS.

Acknowledgments

This paper was sponsored in part by the U.S. Department of Energy's Atmospheric Radiation Measurement (ARM) Program under grant DEFG0294ER61746.

References

- Ellingson, R.G., 1982: On the effects of cumulus dimensions on longwave irradiance and heating rates. *J. of Atmos. Sci.*, **39**:886-896.
- Harshvardhan, and J.A. Weinman, 1982: Infrared radiative transfer through a regular array of cuboidal clouds. *J. of Atmos. Sci.*, **39**:431-439.
- Hu, Y.X., and K. Stamnes, 1993: An accurate parameterization of the radiative properties of water clouds suitable for use in climate models. *J. of Climate*, **6**:728-742.
- Killen, R.M., and R.G. Ellingson, 1994: The effect of shape and spatial distribution of cumulus clouds on longwave irradiance. *J. of Atmos. Sci.*, **51**:2123-2136.
- Takara, E.E., and R.G. Ellingson, 1996: Scattering effects on longwave fluxes in broken cloud fields. *J. of Atmos. Sci.*, **53**:1464-1476.